Article

Not peer-reviewed version

5' DREDGE: Direct Repeat-Enabled Downregulation of Gene Expression via the 5' UTR of Target Genes

Sagar J. Parikh , Heather M. Terron , Luke A. Burgard , Dylan D. Butler , Frank M. LaFerla , Shelley Lane , Malcolm A. Leissring *

Posted Date: 28 April 2025

doi: 10.20944/preprints202504.2190.v1

Keywords: CRISPR; direct repeat; endoribonuclease; gene regulation; RNA interference

 doi:10.20944/preprints202504.2190.v1

Article

5' DREDGE: Direct Repeat-Enabled Downregulation of Gene Expression via the 5' UTR of Target Genes

Sagar J. Parikh [1], Heather M. Terron [1], Luke A. Burgard [1,2], Dylan D. Butler [1,2], Frank M. LaFerla [1,2], Shelley Lane [1] and Malcolm A. Leissring [1,*]

[1] Institute for Memory Impairments and Neurological Disorders, University of California, Irvine, Irvine, CA 92697, USA

[2] Department of Neurobiology and Behavior, University of California, Irvine, Irvine, CA 92697, USA

* Correspondence: m.leissring@uci.edu

Abstract: Despite the availability of numerous methods for controlling gene expression, there remains a strong need for technologies that maximize two key properties: selectivity and reversibility. To this end, we have developed a novel approach that exploits the highly sequence-specific nature of CRISPR-associated endoribonucleases (Cas RNases), which recognize and cleave short RNA sequences known as direct repeats (DRs). In this approach, referred to as DREDGE (direct repeat-enabled downregulation of gene expression), selective control of gene expression is enabled by introducing one or more DRs into the untranslated regions (UTRs) of target mRNAs, which will then be cleaved upon expression of the cognate Cas RNase. We previously demonstrated that the expression of target genes with DRs in their 3' UTRs are efficiently controlled by the DNase-dead version of Cas12a (dCas12a) with a high degree of selectivity and complete reversibility. Here we assess the feasibility of using DREDGE to regulate the expression of genes with DRs inserted within their 5' UTRs. Among five different Cas RNases tested, Csy4 was found to be the most efficient in this format, yielding robust downregulation with rapid onset in doxycycline-regulatable systems targeting either a stably expressed fluorescent protein or an endogenous gene, notably in a fully reversible manner. Unexpectedly, dCas12a was also found to be modestly effective despite binding essentially irreversibly to the cut mRNA on its 5' end and boosting mRNA levels. Our results expand the utility of DREDGE as an attractive method for regulating gene expression in a targeted, highly selective, and fully reversible manner.

Keywords: CRISPR; direct repeat; endoribonuclease; gene regulation; RNA interference

1. Introduction

CRISPR-associated endoribonucleases (Cas RNases) cleave single-stranded RNA in a highly sequence-specific manner by recognizing and binding to short RNA sequences known as direct repeats (DRs) [1–3]. The high degree of specificity of Cas RNases for their cognate DRs suggests that this interaction might be exploited to selectively target and cleave specific mRNAs incorporating one or more DRs. Confirming this, we recently demonstrated that Cas RNases efficiently downregulate target genes incorporating DRs within their 3' untranslated regions (UTRs) [4]. This approach, referred to as 3' DREDGE (direct repeat-enabled downregulation of gene expression), depends on the fact that removal of the poly(A) tail from mRNAs triggers rapid degradation via deadenylation-dependent mRNA decay [4,5]. We found that 3' DREDGE could be implemented by multiple Cas RNases, the most efficient being the DNase-dead version of Cas12a (dCas12a) [4,6]. 3' DREDGE proved to be highly effective, resulting in >90% downregulation of target genes in a manner that was rapid, highly selective, and completely reversible [4].

In the present study, we evaluated the effectiveness of DREDGE to control the expression of genes with DRs incorporated within their 5' UTRs. In this variation, dubbed 5' DREDGE, cleavage of

 doi:10.20944/preprints202504.2190.v1

the DR by the Cas RNase results in separation of the bulk of the mRNA from the 5' portion containing the 7-methylguanosine 5' cap (see Figure 1A) [7]. Removal of the 5' cap, in turn, disrupts translation and triggers mRNA decay via any of several mechanisms. Translation is impaired both because the 5' cap normally facilitates export of mRNA from the nucleus and also because it is critical for interaction with translation initiation factors [8,9]. Uncapped mRNA also decays rapidly through 5'-3' exonucleolytic degradation normally blocked by the 5' cap [10,11].

Here we compare the efficacy of 5' DREDGE implemented with five different Cas RNases and their cognate DRs, identifying Csy4 (also known as Cas6f) as the most effective in a transient transfection paradigm [12]. dCas12a also performed relatively well in this paradigm so was evaluated in parallel. In stable cell lines expressing destabilized green fluorescent protein (GFPd2) with cognate DRs in their 5' UTRs, efficient downregulation was achieved by Csy4, while more modest reductions were obtained by dCas12a. Explaining its poor performance, dCas12a expression was found to dramatically *increase* in GFPd2 mRNA due to its essentially irreversible binding to the downstream 5' end of the cleaved mRNA. Csy4 was subsequently shown to efficiently downregulate an endogenous gene after introduction of a 5' UTR DR via CRISPR-Cas. 5' DREDGE achieved >90% downregulation of the endogenous gene in this format—crucially—in a manner that was fully reversible even after several months of continuous downregulation. Our results establish 5' DREDGE as an effective means to tightly control gene expression, with several advantages over existing technologies.

2. Materials and Methods

2.1. DNA Constructs

All constructs were assembled using the HiFi DNA Assembly Kit according to the manufacturer's recommendations (New England Biolabs (NEB), Beverly, MA, USA) from DNA fragments generated either by restriction digestion, by PCR with Q5® DNA Polymerase (NEB, Beverly, MA, USA), or by de novo DNA synthesis (Integrated DNA Technologies (IDT), San Diego, CA, USA). All constructs were verified by next-generation DNA sequencing (Azenta Life Sciences, Burlington, MA, USA). Source vectors included Addgene plasmids #14760 [13], #155307 [14], #183956 [6], #52119 (gift of Daria Vignali), #183962 [6], and pTet-One [15] (Takara Bio USA, Inc., San Jose, CA, USA). Detailed cloning methods are provided in the Supplemental Information.

2.2. Cell Culture

All experiments employed wild-type, SV40-immortalized mouse embryonic fibroblasts (MEFs; Cat #CRL-2907; ATCC, Manassas, VA, USA). Cells were maintained at 37 °C in a humidified incubator supplemented with 5% CO_2 in DMEM containing GlutaMAX® supplemented with 10% Tet System Approved Fetal Bovine Serum (Takara Bio USA, San Jose, CA, USA), 100 U/mL penicillin, and 100 µg/mL streptomycin.

2.3. Flow Cytometry and FACS

For the screening of Cas RNases, MEFs were transfected with expression vectors using the Amaxa Nucleofector II electroporation system according to the manufacturer's recommendation (Lonza Bioscience, Bend, OR, USA) and cultured overnight. Cells were then imaged on a Zeiss Axiovert 200 m fluorescent microscope (Zeiss, Dublin, CA, USA), harvested by trypsinization, and collected in tubes via a cell strainer. Flow cytometry on these cells and subsequently generated stable cell lines was performed on a BD LSRFortessa™ X-20 Cell Analyzer using lasers and filter sets optimized for the detection of GFP and mCherry fluorescence according to manufacturer's recommendations (BD BioSciences, Franklin Lakes, NJ, USA). For the generation of stable cell lines, individual cells were plated into 96-well plates by fluorescence-activated cell sorting (FACS) using a BD FACSAria™ II Cell Sorter (BD BioSciences, Franklin Lakes, NJ, USA).

 doi:10.20944/preprints202504.2190.v1

2.4. mRNA Collection and Analyses

Total mRNA from double-stable cell lines homogenized with QIAshredder™ was purified using RNeasy Plus Mini Kit, according to the manufacturer's recommendations (QIAGEN, LLC, Germantown, MD, USA). Quantitative real-time PCR (RT-PCR) was performed on a CFX96 Touch Real-Time PCR Detection System using reagents from the SingleShot™ SYBR® Green One-Step Kit according to the manufacturer's recommendations (Bio-Rad, Hercules, CA, USA). Primer pairs (Fwd, Rev) were: GFP-A (ATGTCTTGTGCCCAGGAGAG, GTGGTATTTGTGAGCCAGGG) and GAPDH (CCCACTCTTCCACCTTCGAT, GAGTTGGGATAGGGCCTCTC).

2.5. Targeted Modification of the CTSD Locus

The Csy4 DR was introduced into the 5' UTR of the endogenous *CTSD* locus of MEFs using a de novo synthesized targeting construct containing: (1) the Csy4 DR within Exon 1 of CTSD; (2) a cassette expressing puromycin resistance ($Puro^r$) under the control of the PGK promoter within the first intron, flanked by FRT sites to permit its removal with Flp-recombinase; and (3) ~600 bp 5' and 3' homology arms (see Figure 4 and Supplementary Figure S1B; GenScript USA, Piscataway, NJ, USA). For CRISPR-Cas, cells were transfected as above with a mixture comprising: (1) recombinant Alt-R A.s. Cas12a (Cpf1) *Ultra* Nuclease; (2) two synthetic gRNAs (GGGAGUCUUCAUGGUCGCGG and ACCUGGAGUGCCGCGUGCUC); and (3) 0.5 μg of a PCR product amplified from the targeting construct generated using two oligonucleotides (Fwd, C*A*TTGCTACATTATGGAATG-TGCATG; Rev, C*A*CCAAGACCTCATCTAGCAC), where asterisks indicate the placement of phosphorothioate bonds incorporated to inhibit degradation of the amplicon (IDT, San Diego, CA, USA). After selection of Puro-resistant cells and identification of positive clones, the $Puro^r$ cassette was removed by transfecting cells with pCAG-Flpe:GFP (Addgene Plasmid #13788) [13]. Two days after transfection, individual GFP-positive were isolated by cell sorting, then screened by PCR to confirm removal of the $Puro^r$ cassette.

2.6. CatD Activity Assays

CatD activity assays were performed on cell lysates using the fluorogenic peptide substrate, Mca-GKPILFFRLK(Dnp)-R-NH_2 (InnoPep, Inc. San Diego, CA, USA), by continuous monitoring of increases in fluorescence (λ_{ex} = 328 nm, λ_{em} = 393 nm) as a function of time, as described [4,16,17]. Relative rates of CatD activity were obtained from the slopes of linear portions of progress curves and normalized to protein concentrations quantified by A280 measurements using a NanoDrop® ND-1000 UV-Vis Spectrophotometer (Thermo Fisher Scientific, Waltham, MA, USA).

 doi:10.20944/preprints202504.2190.v1

3. Results

3.1. Selection and Screening of Candidate Cas RNases for 5′ DREDGE

To assess the feasibility of regulating gene expression using the 5′ DREDGE approach (Figure 1A), five different Cas RNases were selected for investigation (Figure 1B). Cas12a from *Lachnospiraceae bacterium* (also known as Cpf1; Figure 1B) was chosen because it proved to be the top candidate for 3' DREDGE [4]. Cas12a is an atypical Cas RNase because it also possesses DNase activity; we therefore utilized a DNase-dead version, in particular the "hyperdCas12a" version engineered by Guo and colleagues [6]. For the Cas12a DR, we also included a short A/U-rich "synthetic separator" (synSeparator; Figure 1B)—AAAU—which promotes excision of spacer sequences when placed adjacent to the 5′ end of the Cas12a DR [18] (Figure 1B). PfCas6 from *Pyrococcus furiosus* and SsoCas6 from *Sulfolobus solfataricus* (Figure 1B) were selected because they are "multiple-turnover enzymes" in contradistinction to single-turnover Cas RNases that remain bound to the cognate DR after cleavage [2]. Lastly, CasE (also known as EcoCas6e) and Csy4 (also known as Cas6f)—from *Escherichia coli* and *Pseudomonas aeruginosa*, respectively—were chosen based on a study reporting these as the top-performing Cas RNases among nine tested when present in mRNAs [19].

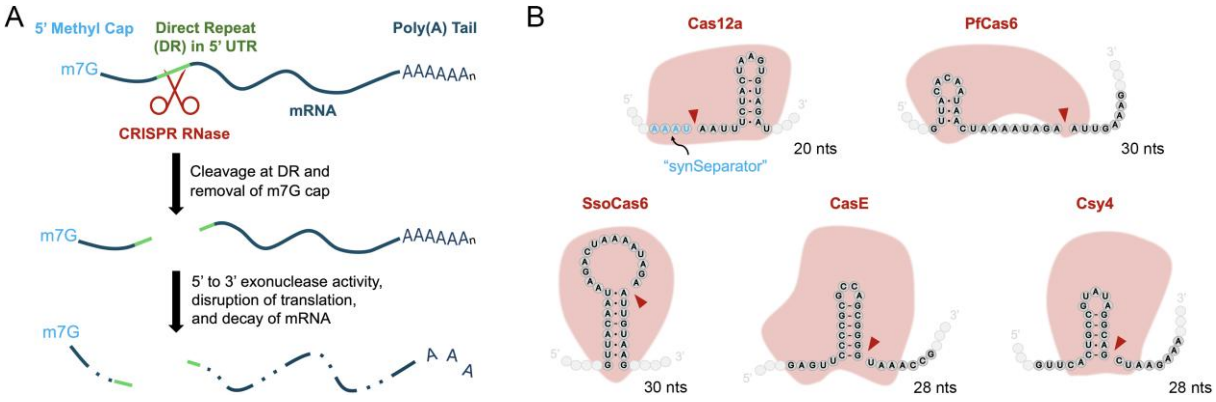

Figure 1. Candidate Cas RNases for 5′ DREDGE. (**A**) Mechanism of 5′ DREDGE. Cleavage of the DR(s) within the 5′ UTR of mRNA (green) by a Cas RNase (red) removes the 7-methylguanosine (m7G) 5' cap, causing impairments in translation by multiple mechanisms as well as degradation by 5'-3' exonuclease activity (see text). (**B**) DRs for the five Cas RNases investigated in this study, with cleavage sites indicated (red arrows) along with sizes in nucleotides (nts). Note the "synSeparator" adjacent to the 5′ end of the Cas12a DR.

The cognate DRs of the five Cas RNases (Figure 1B) are all quite short, comprising ≤30 nucleotides, but highly varied in primary nucleotide sequence (Figure 1B). Of note, all Cas RNases except Cas12a cleave within the DR at a position close to the 3′ end, whereas Cas12a cleaves outside the DR, at the 5′ end.

The five selected Cas RNases were assessed for their ability to downregulate a target gene using a two-part model system that incorporates GFP fluorescence as a convenient marker of target gene expression and mCherry as a marker of Cas RNase expression (Figure 2A). The first part comprised vectors expressing a destabilized form of GFP (GFPd2) with a short, two-hour half-life ($t_{1/2}$) [13]. One DR for each of the five Cas RNases was cloned into the 5′ UTR of this construct, with the parental vector serving as a "No-DR" control (Figure 2A, top). The second part of this system relied on a vector expressing mCherry via an internal ribosomal entry site, into which was cloned each of the five Cas RNases, including versions either lacking or containing a nuclear localization signal (NLS) (two in the case of Cas12a) for a total of 10 Cas RNase expression constructs plus the parent vector, which served as a "No-RNase" control (Figure 2A, bottom).

 doi:10.20944/preprints202504.2190.v1

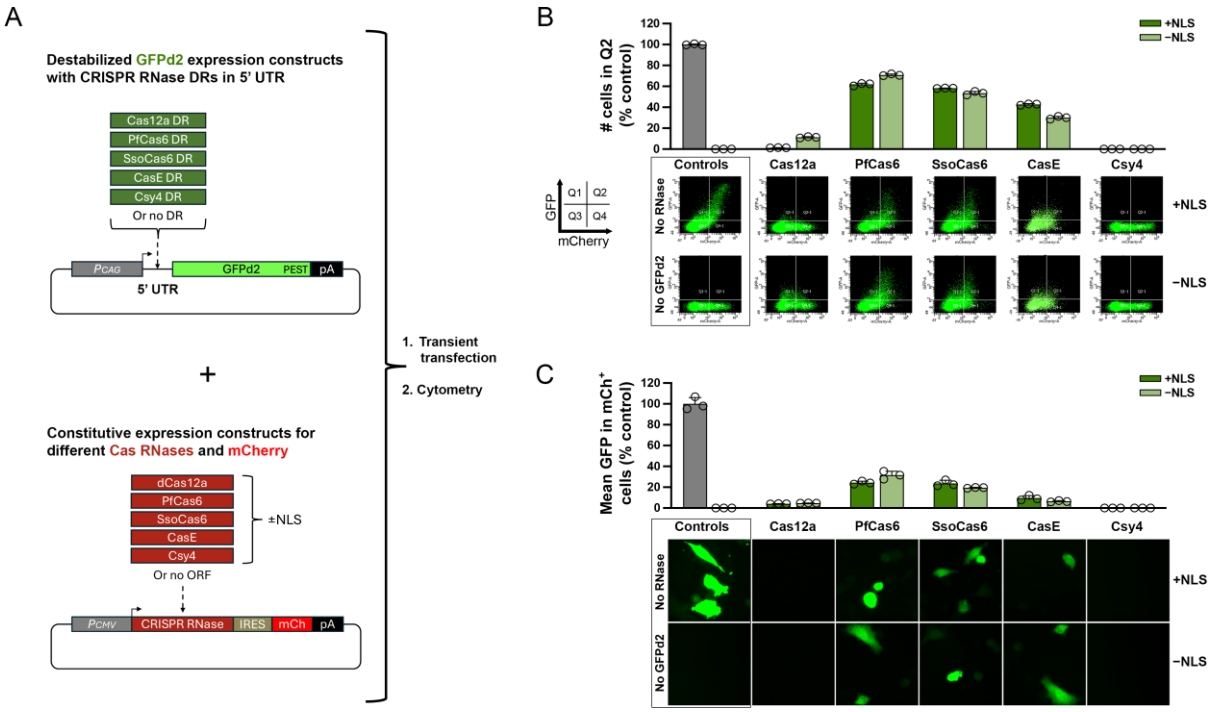

Figure 2. Screening of candidate Cas RNases for 5′ DREDGE. (**A**) Designs of constructs expressing GFPd2 with different DRs (or no DR) in the 5′ UTR (green) and constructs expressing individual Cas RNases (or no RNase) together with mCherry (red). (**B**) Cell cytometry data for MEFs expressing different Cas RNases and GFPd2 constructs with their cognate DRs. Graph of the percentage of cells in Q2 relative to controls (top) within log-log plots of GFP vs. mCherry RFU values (n = 3 replicates), with representative plots shown (bottom). (**C**) Graph of GFP intensity in mCherry+ cells derived from RFU plots shown in (**B**) and normalized to controls, along with representative images of GFP fluorescence in cells prior to cytometry (bottom).

To assess the relative efficacy of the different RNases, MEFs were cotransfected with each Cas RNase/mCherry construct along with the GFPd2 construct harboring the cognate DR(s) in its 5′ UTR, then analyzed by cell cytometry one day later. Log-log plots of mCherry and GFP fluorescence, on the X- and Y-axes, respectively, were generated and subdivided into four quadrants by the boundaries for GFP and mCherry fluorescence (Figure 2B). In control cells cotransfected with No-DR GFPd2 and No-RNase mCherry, abundant GFP and mCherry fluorescence were present, resulting in large numbers of cells appearing in the upper-right quadrant (Q2) of RFU plots; conversely, for cells expressing mCherry alone, no cells were present in Q2, as expected (Figure 1B). Relative to No-RNase controls, cells expressing each of the five Cas RNases and their cognate DRs all showed decreases in the percentage of cells in Q2 to varying extents (Figure 1B), together with more substantial reductions in the mean level of GFP fluorescence in mCherry-positive cells (e.g., cells in Q2 and Q4; Figure 1C). Significantly, Csy4 performed superiorly relative to all other Cas RNases tested by both metrics, with almost no cells appearing in Q2 (Figure 2B) and GFP fluorescence levels being indistinguishable from No-GFPd2 controls (Figure 2C). dCas12a performed comparably, albeit with some notable differences. In particular, whereas essentially no cells were present in Q2 for cells expressing dCas12 with two NLSs, the version lacking an NLS did not achieve complete downregulation (Figure 2B). Also, both versions of dCas12a failed to achieve complete downregulation as assessed by mean GFP fluorescence (Figure 2C). Given the comparatively poor performance of 5' DREDGE with the other Cas RNases (Figure 2B,C), we elected to proceed with more thorough evaluation of dCas12a and Csy4, both possessing NLS sequences.

 doi:10.20944/preprints202504.2190.v1

3.2. Dox-Regulatable Gene Expression by 5′ DREDGE Using dCas12a and Csy4

We next sought to characterize the performance of cells expressing dCas12a or Csy4 in a doxycycline (Dox)-dependent manner, using the Tet-One™ system [15] (Takara Bio USA, Inc., San Jose, CA, USA). To that end, we first created cell lines stably expressing GFPd2 with either one Cas12 or one Csy4 DR in the 5' UTR, or no DR as a negative control (Figure 3A). These stable cell lines were subsequently used to generate double-stable lines also expressing dCas12a or Csy4 together with mCherry and neomycin resistance, all under the control of the TRE promoter to permit Dox-regulatable expression (Figure 3B). The latter construct lacking a Cas RNase served as a No-RNase control. As illustrated in Figure 3C,D, all control lines performed as anticipated. For the No-DR GFPd2 cells lines, essentially 0% and 100% of cells appeared in Q2 in the absence or presence of Dox, respectively, whether expressing dCas12a, Csy4, or no RNase (Figure 3C, left), and mean GFP levels were essentially unchanged, irrespective of RNase expression or Dox administration (Figure 3D, left). Cells stably expressing GFPd2 with either one Cas12a DR or one Csy4 DR in the 5′ UTR behaved similarly in the presence of Dox (1 μg/mL) when co-expressing the No-RNase Dox-inducible control vector (Figure 3C,D, middle). Contrary to the substantial downregulation achieved with dCas12a in the transient transfection paradigm (Figure 2B,C), Dox-induced expression of dCas12a in the GFPd2 line with its cognate DR elicited only a very modest (~6%) reduction in the number of cells in Q2. In marked contrast, expression of Csy4 in the GFPd2 line with the Csy4 DR elicited substantial reductions in the same metric (73.2%) relative to the same parental lines expressing No-RNase mCherry controls (Figure 3C, right). In terms of mean GFP fluorescence (Figure 3D), cells with Dox-induced dCas12a or Csy4 expression exhibited 72.8% and 85.5% reductions, respectively (Figure 3D, middle and right). Thus, whereas Csy4 performed well for 5' DREDGE on both metrics, dCas12a appeared to achieve a moderate but relatively uniform decrease in GFP fluorescence in the majority of GFP-expressing cells, with very few cells exhibiting complete downregulation.

To more completely characterize the performance of 5′ DREDGE with these two Cas RNases, we used these stable lines to carry out Dox dose-response experiments (Figure 3E,F) as well as time courses of the responsiveness of gene expression after the addition or removal of Dox (Figure 3G). Dose-response experiments conducted in the cell lines with one Csy4 DR yielded IC_{50} of 143 ng/mL Dox using the percent of mCherry-positive cells (Q2 + Q4) present in Q2 as a metric (Figure 3E), and similar results were obtained using mean GFP fluorescence in all cells, yielding an IC_{50} of 242 ng/mL Dox (Figure 3F). dCas12a performed less well, yielding an IC_{50} of 602 ng/mL Dox by the latter metric (Figure 3F); by the former metric, however, its performance was so poor as to preclude calculation of an IC_{50} value (Figure. 3E). Consistent with the results obtained for 3' DREDGE [4], time courses revealed that the 5′ DREDGE approach exhibits notably fast kinetics, particularly for Csy4. The $t_{1/2}$s for induction of downregulation by addition of Dox were 0.56 for Csy4, but 1.8 d for dCas12a; by contrast, the $t_{1/2}$s for restoration of activity after withdrawal of Dox were both remarkably fast: 0.31 and 0.35 d, respectively (Figure 3G).

Finally, we quantified GFPd2 mRNA levels by real-time PCR (RT-PCR) in these double-stable lines in the absence vs. the presence of Dox. Addition of Dox to the Csy4 line resulted in a 75% reduction in GFPd2 mRNA (Figure 3I), a figure perfectly in line with the magnitude of the reduction in GFPd2 expression quantified by cell cytometry (Figure 3C,D). In a dramatic contradistinction, induction of dCas12a expression by Dox resulted in a remarkable 16-fold *increase* in GFPd2 mRNA (Figure 3H). This intriguing finding helps to explain the comparatively poor performance of this Cas RNase in 5' DREDGE, as discussed in greater depth in Section 4.

 doi:10.20944/preprints202504.2190.v1

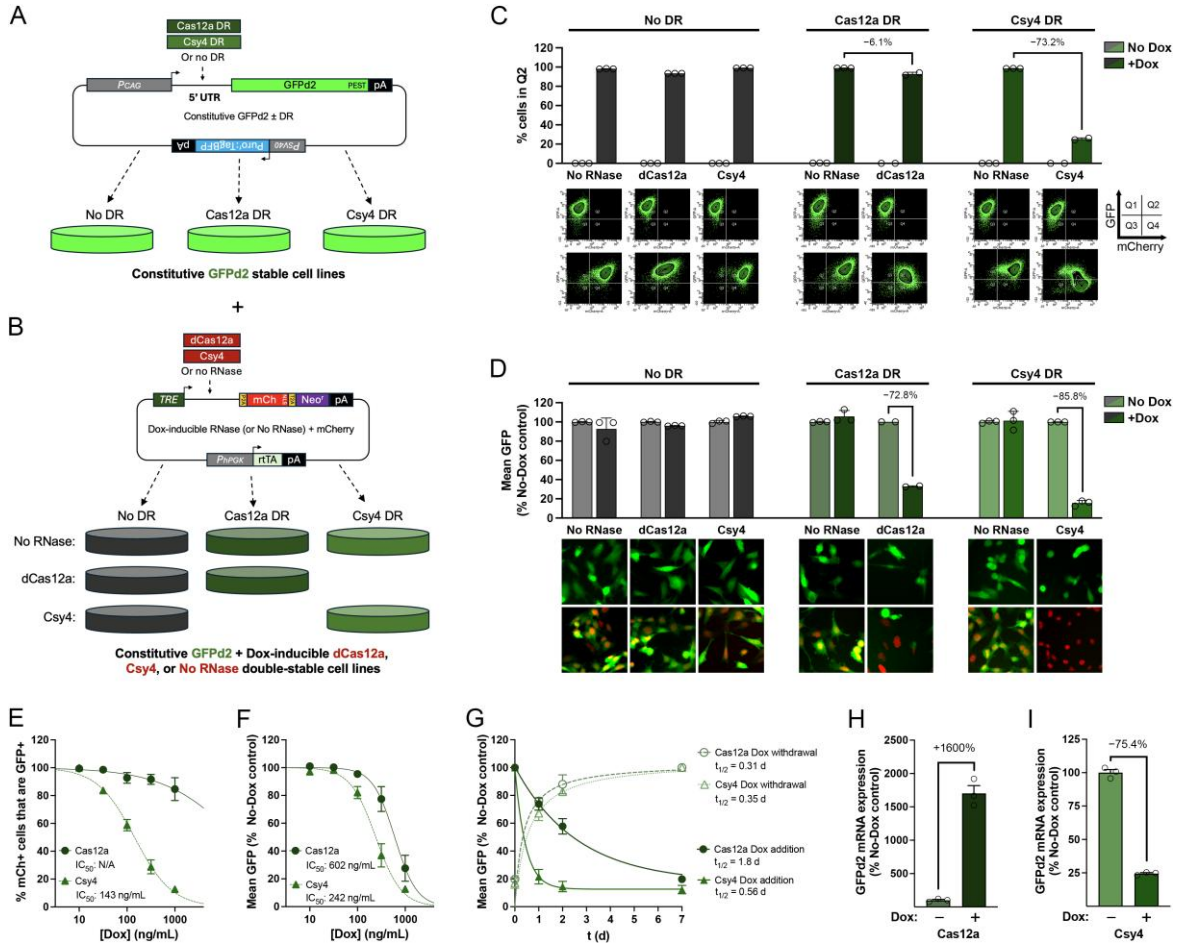

Figure 3. Dox-regulatable control of gene expression by 5′ DREDGE. (**A**) Design of constructs constitutively expressing GFPd2 with no DR or one Cas12a DR or one Csy4 DR in the 5′ UTR, which were used to create three different stable cell lines. (**B**) Design of constructs with Dox-regulatable co-expression of dCas12a or Csy4 (or No RNase) and mCherry used to create double-stable cell lines from the lines in (**A**). (**C**) Percentage of cells in Q2 for double-stable cell lines conditionally expressing either no RNase, dCas12a, or Csy4, tested in the absence or presence of Dox, together with GFPd2 constructs containing no DR (left) or the cognate DRs for Cas12a (middle) or Csy4 (right), as derived from log-log plots of GFP vs. mCherry RFU (bottom). (**D**) Mean GFP RFU in the cell lines in (**C**) in the absence or presence of Dox derived from cell cytometry (top) with representative images of cells in the different conditions (bottom). Data in (**C**) and (**D**) are normalized to Dox-treated No-DR and No-RNase controls; n = 2–3 per condition. (**E**,**F**) Dox dose-response experiments from double-stable cell lines with one Cas12a or one Csy4 DR in the 5' UTR conditionally expressing the cognate Cas RNases. Graphs show responsiveness to different concentrations of Dox in terms of (**E**) the percent of mCherry-positive cells (i.e., Q2 + Q4) that were also GFP-positive (i.e., in Q2) and (**F**) mean GFP RFU. Mean IC_{50} values for all dose-response experiments are indicated. Data are mean ± SEM, normalized to values in the absence of Dox for each line; n = 2–3 per condition. (**G**) Time courses of GFP RFU in response to addition (solid lines) or withdrawal (dashed lines) of Dox in the cell lines in (**E**) and (**F**) normalized to No-Dox controls. Mean $t_{1/2}$ values are shown. Data are mean ± SEM for 2–3 independent experiments. (**H**,**I**) Relative expression of GFPd2 mRNA in the absence versus the presence of Dox in double-stable cell lines instantiating 5' DREDGE with Cas12a (**H**) and Csy4 (**I**). Note the dramatic increase in GFPd2 mRNA triggered by dCas12a expression (**H**).

3.3. Dox-Regulatable Downregulation of the Endogenous Gene, CTSD, by 5′ DREDGE

We next sought to assess the feasibility of downregulating an endogenous gene with the 5′ DREDGE approach, specifically the gene for cathepsin D (*CTSD*), which we have targeted with two other technologies, including 3' DREDGE [4,17]. We used a multi-step approach in add a Csy4 DR into the 5′ UTR of *CTSD* then create a stable line expressing Csy4 in a Dox-inducible manner (Figure

 doi:10.20944/preprints202504.2190.v1

4; Supplementary Figure S1). First, we used CRISPR-Cas9 to insert a targeting construct containing a single Csy4 DR within the 5′ UTR of *CTSD* (positioned immediately upstream of the Kozak consensus sequence) together with a Puro^r cassette flanked by FRT sites (positioned within the first intron) (Figure 4B; Supplementary Figure S1B). Second, after identification of a positive clone homozygous for this knockin construct (Supplementary Figure S1), we removed the Puro^r cassette in this line using Flp-recombinase (Figure 4C). Finally, after identification of a cell line with successful removal of the Puro^r cassette, we used the Dox-regulatable constructs expressing either Csy4 or no RNase (and mCherry) to generate stable cell lines (Figure 4D). Multiple individual clones for each line were generated, which behaved as expected: as assessed by CatD activity assays, addition of Dox produced substantial >90% decreases in CatD levels in cells expressing Csy4 in four different cell lines, whereas no decreases were triggered by Dox in the No-RNase controls (Figure 4D). Importantly, CatD activity within these lines in the absence of Dox was comparable to control lines expressing No-RNase control vectors, whether treated with Dox or not, even after extensive incubation with Dox (for ~2 months) during the selection of these lines. Finally, to more completely assess the reversibility of 5' DREDGE, we subjected one of the Csy4-expressing clones to multiple successive alternating treatments without or with Dox, spaced approximately one week apart; as shown in Figure 4E, this line exhibited complete reversibility even after six rounds of Dox changes.

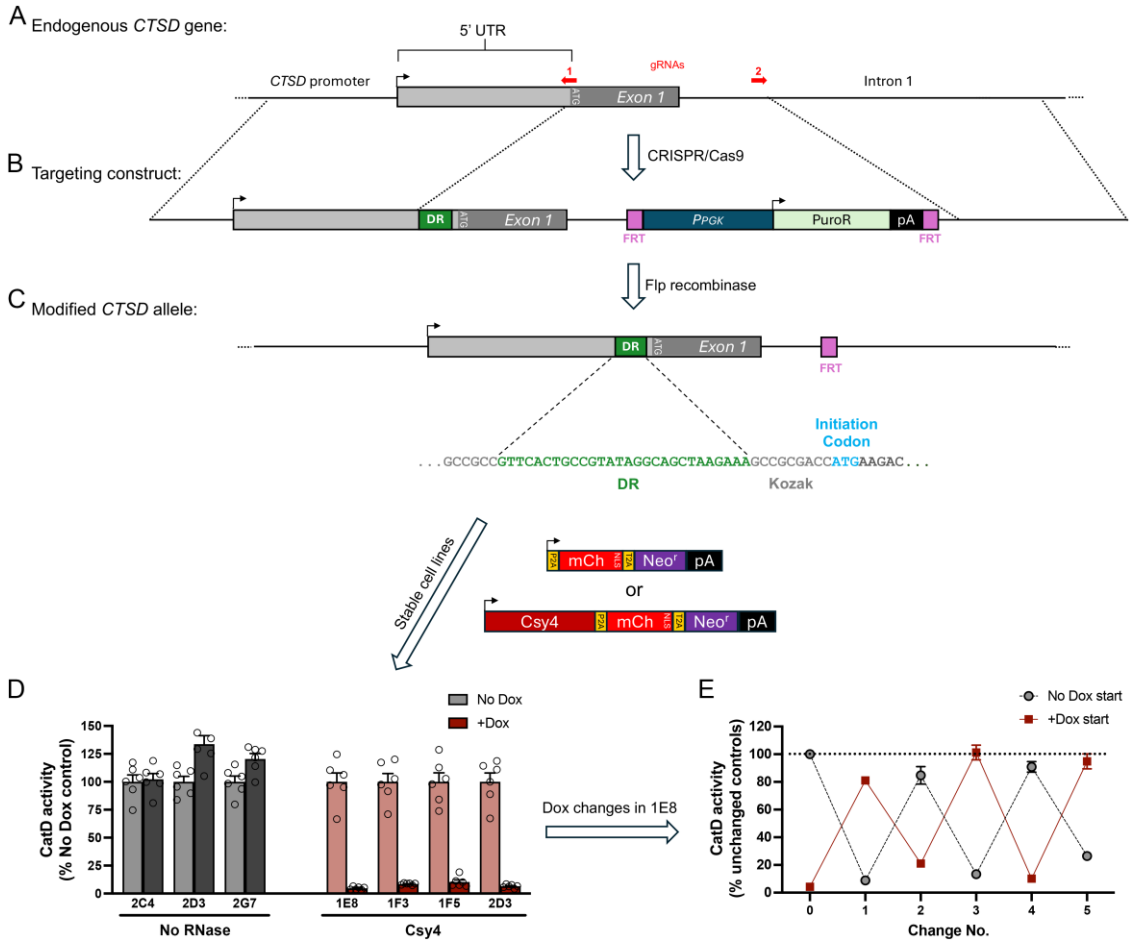

Figure 4. Dox-regulatable control of endogenous *CTSD* expression by 5′ DREDGE. (**A**) Genomic structure of the 5′ end of murine *CTSD*. (**B**) Design of the targeting construct used to insert one Csy4 DRs into the 5′ UTR together with a Puro^r resistance cassette within the first intron of *CTSD*. Note the presence of two FRT sites flanking the Puro^r resistance cassette. (**C**) Structure of the modified *CTSD* allele after removal of Puro^r resistance cassette with Flp-recombinase. The complete sequence of the Csy4 DR is shown (green), highlighting its location relative to the initiation codon (blue). One line with sequence-verified insertion of the Csy4 DR was transfected with the indicated constructs to generate individual stable lines expressing Csy4 or no RNase in a Dox-regulatable

 doi:10.20944/preprints202504.2190.v1

manner. (**D**) CatD activity in the latter stable lines in the presence of Dox (1 μg/mL) relative to no Dox. Data are mean ± SEM; n = 5 - 6. (**E**) CatD proteolytic activity in stable line 1E8 subjected to repeated changes from +Dox to no Dox and vice versa spaced ~1 week apart. Data are mean ± SEM; n = 8 replicates per condition.

4. Discussion

Our group conceived of the general approach of DREDGE as a novel means to achieve targeted downregulation of genes in a fully reversible manner, with the explicit goal of evaluating its suitability for in vivo applications [16,20,21]. As our recent analysis demonstrated [4], 3' DREDGE implemented with dCas12a yields robust downregulation of target genes with rapid kinetics, crucially in a manner that is both highly selective and completely reversible. The present study extends this work, establishing that DREDGE can also be implemented by incorporation of a Cas RNase DR within the 5' UTR of target genes. In this case, Csy4 was found to be the most effective for 5' DREDGE among five Cas RNases tested, performing comparably to 3' DREDGE implemented with dCas12a when used to target both a stably expressed protein and an endogenous gene [4]. Csy4 is an ideal Cas RNase for another reason: the Csy4:DR interaction, with a ~50 pM equilibrium dissociation constant, constitutes one of the highest-affinity protein:RNA interactions yet identified [12].

Unexpectedly, our initial screening of candidate Cas RNases using a transient transfection paradigm suggested that dCas12a might also be effective for 5' DREDGE. This was surprising given that dCas12a is well-established to remain tightly bound to RNA after cleavage on the 5' end of the DR (Figure 1B) [22–24]. Further assessment, however, revealed that dCas12a performed poorly in stable cell lines as compared both to Csy4 and to the transient transfection paradigm. Moreover, consistent with the essentially irreversible interaction between dCas12a and its cognate DR, mRNA levels of the target gene in stable cells were found to be markedly increased when dCas12a expression was induced for several days. These findings suggest, on the one hand, that binding of dCas12a to the cognate mRNA disrupts translation of the bound mRNA. This might occur due to any of several mechanisms. For instance, because the 5' cap is critical for export of mRNA to the cytosol [9], it seems reasonable that removal of the cap by dCas12a impairs this process. This explanation is supported by the observation that dCas12a lacking a NLS performed less well in the transient transfection paradigm as compared to the version with two NLSs (c.f., Figure 2B). Another plausible mechanism may involve reduced translation of the dCas12a-bound mRNA due to impaired interaction with translation initiation factors that depend upon the presence of the 5' cap [8]. Finally, we speculate that the dCas12a protein itself might also inhibit translation, possibly by steric blockade of the mRNA from productive engagement with the ribosome. On the other hand, binding of the mRNA also prevents decay of the mRNA, increasing its levels over time and thus acting as a countervailing influence on the degree of translation of the target gene. In the transient transfection paradigm, assessed just 24 hours later, mRNA accumulation likely did not occur to the same extent, thus explaining the enhanced downregulation of the target gene by dCas12a in this context. Most or all of these mechanisms are likely to be operative simultaneously and to varying degrees. While they help to account for the unexpected behavior of dCas12a, given the poor performance of this Cas RNase in 5' DREDGE, there seems to be scant rationale for further elucidation of the underlying mechanisms.

5. Conclusions

Our results establish 5' DREDGE as an effective method for achieving reversible downregulation of target genes, with several unique advantages. Only minimal modification to the 5' UTR of the target gene is necessary—the addition of just 28 nucleotides in the case of the Csy4 DR—thus minimizing the potential for interference with transcription or translation or interactions with *trans*-acting elements such as microRNAs [25]. More-over, by contrast to RNAi and CRISPRi, which rely upon RNA:RNA and RNA:DNA complementarity that can tolerate mismatches to varying degrees, the reliance of 5' DREDGE on a non-mammalian *cis*-element, together with the high-specificity and high-affinity Csy4 protein:RNA interaction [12], greatly reduces the risk of off-target effects. In sum,

 doi:10.20944/preprints202504.2190.v1

our results demonstrate that 5' DREDGE constitutes a viable alternative for achieving the controlled regulation of target genes, one that is particularly well suited to applications requiring efficient downregulation, high selectivity, and complete reversibility.

Supplementary Materials: The following supporting information can be downloaded at: Preprints.org, Figure S1: Overview of genotyping results confirming the successful introduction of one Csy4 DR into the 5' UTR of murine *CTSD* via CRISPR-Cas.

Author Contributions: Conceptualization, M.A.L.; methodology, M.A.L.; validation, S.J.P., H.M.T., L.A.B., D.D.B., S.L., and M.A.L.; data analysis, S.J.P., H.M.T., S.L., and M.A.L.; investigation, S.J.P., H.M.T., L.A.B., D.D.B., S.L., and M.A.L.; resources, F.M.L. and M.A.L.; writing—original draft preparation, M.A.L.; writing—review and editing, S.J.P. and S.L.; supervision, F.M.L., S.L., and M.A.L.; funding acquisition, F.M.L. and M.A.L. All authors have read and agreed to the published version of the manuscript.

Funding: This research was funded by the U.S. National Institutes of Health Grant No. R01 AG066928 to F.M.L. and M.A.L.

Institutional Review Board Statement: Not applicable.

Informed Consent Statement: Not applicable.

Data Availability Statement: Data are contained within the article and Supplementary Material. Original, raw fluorescence microscopy image files are deposited at the Open Science Framework repository, available at: www.doi.org/10.17605/OSF.IO/EUV7H (accessed on 24 April 2025).

Acknowledgments: The authors thank the laboratory of Jorge Busciglio for generously providing access to their multiplate reader. We are grateful to Pauline Nguyen for expert assistance with cell cytometry and FACS analysis within the UCI Stem Cell Research Center. We thank Connie Cepko, Stanley L. Qi, Luke A. Gilbert, and Dario Vignali for providing cloning vectors via Addgene.

Conflicts of Interest: The authors declare no conflicts of interest.

References

1. Charpentier, E., H. Richter, J. van der Oost, and M. F. White. "Biogenesis pathways of RNA guides in archaeal and bacterial CRISPR-Cas adaptive immunity." FEMS Microbiol Rev 39, no. 3 (2015): 428-41. https://doi.org/10.1093/femsre/fuv023
2. Hochstrasser, M. L., and J. A. Doudna. "Cutting it close: CRISPR-associated endoribonuclease structure and function." Trends Biochem Sci 40, no. 1 (2015): 58-66. https://doi.org/10.1016/j.tibs.2014.10.007
3. Wiedenheft, B., S. H. Sternberg, and J. A. Doudna. "RNA-guided genetic silencing systems in bacteria and archaea." Nature 482, no. 7385 (2012): 331-8. https://doi.org/10.1038/nature10886
4. Parikh, S. J., H. M. Terron, L. A. Burgard, D. S. Maranan, D. D. Butler, A. Wiseman, F. M. LaFerla, S. Lane, and M. A. Leissring. "Targeted control of gene expression using CRISPR-associated endoribonucleases." Cells 14, no. 7 (2025). https://doi.org/10.3390/cells14070543
5. Chen, C. Y., and A. B. Shyu. "Mechanisms of deadenylation-dependent decay." Wiley Interdiscip Rev RNA 2, no. 2 (2011): 167-83. https://doi.org/10.1002/wrna.40
6. Guo, L. Y., J. Bian, A. E. Davis, P. Liu, H. R. Kempton, X. Zhang, A. Chemparathy, B. Gu, X. Lin, D. A. Rane, X. Xu, R. M. Jamiolkowski, Y. Hu, S. Wang, and L. S. Qi. "Multiplexed genome regulation in vivo with hyper-efficient Cas12a." Nat Cell Biol 24, no. 4 (2022): 590-600. https://doi.org/10.1038/s41556-022-00870-7
7. Avila-Bonilla, R. G., and S. Macias. "The molecular language of RNA 5' ends: guardians of RNA identity and immunity." RNA 30, no. 4 (2024): 327-36. https://doi.org/10.1261/rna.079942.124
8. Borden, K. L. B., and L. Volpon. "The diversity, plasticity, and adaptability of cap-dependent translation initiation and the associated machinery." RNA Biol 17, no. 9 (2020): 1239-51. https://doi.org/10.1080/15476286.2020.1766179

 doi:10.20944/preprints202504.2190.v1

9. Mars, J. C., B. Culjkovic-Kraljacic, and K. L. B. Borden. "eIF4E orchestrates mRNA processing, RNA export and translation to modify specific protein production." Nucleus 15, no. 1 (2024): 2360196. https://doi.org/10.1080/19491034.2024.2360196
10. He, F., and A. Jacobson. "Eukaryotic mRNA decapping factors: molecular mechanisms and activity." FEBS J 290, no. 21 (2023): 5057-85. https://doi.org/10.1111/febs.16626
11. Kramer, S., and A. G. McLennan. "The complex enzymology of mRNA decapping: Enzymes of four classes cleave pyrophosphate bonds." Wiley Interdiscip Rev RNA 10, no. 1 (2019): e1511. https://doi.org/10.1002/wrna.1511
12. Sternberg, S. H., R. E. Haurwitz, and J. A. Doudna. "Mechanism of substrate selection by a highly specific CRISPR endoribonuclease." RNA 18, no. 4 (2012): 661-72. https://doi.org/10.1261/rna.030882.111
13. Matsuda, T., and C. L. Cepko. "Controlled expression of transgenes introduced by in vivo electroporation." Proc Natl Acad Sci U S A 104, no. 3 (2007): 1027-32. https://doi.org/10.1073/pnas.0610155104
14. Abbott, T. R., G. Dhamdhere, Y. Liu, X. Lin, L. Goudy, L. Zeng, A. Chemparathy, S. Chmura, N. S. Heaton, R. Debs, T. Pande, D. Endy, M. F. La Russa, D. B. Lewis, and L. S. Qi. "Development of CRISPR as an Antiviral Strategy to Combat SARS-CoV-2 and Influenza." Cell 181, no. 4 (2020): 865-76 e12. https://doi.org/10.1016/j.cell.2020.04.020
15. Loew, R., N. Heinz, M. Hampf, H. Bujard, and M. Gossen. "Improved Tet-responsive promoters with minimized background expression." BMC Biotechnol 10 (2010): 81. https://doi.org/10.1186/1472-6750-10-81
16. Suire, C. N., S. O. Abdul-Hay, T. Sahara, D. Kang, M. K. Brizuela, P. Saftig, D. W. Dickson, T. L. Rosenberry, and M. A. Leissring. "Cathepsin D regulates cerebral Abeta42/40 ratios via differential degradation of Abeta42 and Abeta40." Alzheimers Res Ther 12, no. 1 (2020): 80. https://doi.org/10.1186/s13195-020-00649-8
17. Terron, H. M., D. S. Maranan, L. A. Burgard, F. M. LaFerla, S. Lane, and M. A. Leissring. "A dual-function "TRE-Lox" system for genetic deletion or reversible, titratable, and near-complete downregulation of cathepsin D." Int J Mol Sci 24, no. 7 (2023). https://doi.org/10.3390/ijms24076745
18. Magnusson, J. P., A. R. Rios, L. Wu, and L. S. Qi. "Enhanced Cas12a multi-gene regulation using a CRISPR array separator." Elife 10 (2021). https://doi.org/10.7554/eLife.66406
19. Campa, C. C., N. R. Weisbach, A. J. Santinha, D. Incarnato, and R. J. Platt. "Multiplexed genome engineering by Cas12a and CRISPR arrays encoded on single transcripts." Nat Methods 16, no. 9 (2019): 887-93. https://doi.org/10.1038/s41592-019-0508-6
20. Terron, H. M., S. J. Parikh, S. O. Abdul-Hay, T. Sahara, D. Kang, D. W. Dickson, P. Saftig, F. M. LaFerla, S. Lane, and M. A. Leissring. "Prominent tauopathy and intracellular beta-amyloid accumulation triggered by genetic deletion of cathepsin D: implications for Alzheimer disease pathogenesis." Alzheimers Res Ther 16, no. 1 (2024): 70. https://doi.org/10.1186/s13195-024-01443-6
21. Suire, C. N., and M. A. Leissring. "Cathepsin D: A candidate link between amyloid beta-protein and tauopathy in Alzheimer disease." J Exp Neurol 2, no. 1 (2021): 10-15. https://doi.org/10.33696/Neurol.2.029
22. Chen, J., X. Lin, W. Xiang, Y. Chen, Y. Zhao, L. Huang, and L. Liu. "DNA target binding-induced pre-crRNA processing in type II and V CRISPR-Cas systems." Nucleic Acids Res 53, no. 3 (2025). https://doi.org/10.1093/nar/gkae1241
23. Dong, D., K. Ren, X. Qiu, J. Zheng, M. Guo, X. Guan, H. Liu, N. Li, B. Zhang, D. Yang, C. Ma, S. Wang, D. Wu, Y. Ma, S. Fan, J. Wang, N. Gao, and Z. Huang. "The crystal structure of Cpf1 in complex with CRISPR RNA." Nature 532, no. 7600 (2016): 522-6. https://doi.org/10.1038/nature17944
24. Sinan, S., N. M. Appleby, C. W. Chou, I. J. Finkelstein, and R. Russell. "Kinetic dissection of pre-crRNA binding and processing by CRISPR-Cas12a." RNA 30, no. 10 (2024): 1345-55. https://doi.org/10.1261/rna.080088.124
25. O'Brien, J., H. Hayder, Y. Zayed, and C. Peng. "Overview of microRNA biogenesis, mechanisms of actions, and circulation." Front Endocrinol (Lausanne) 9 (2018): 402. https://doi.org/10.3389/fendo.2018.00402

 doi:10.20944/preprints202504.2190.v1

disclaim responsibility for any injury to people or property resulting from any ideas, methods, instructions or products referred to in the content.